X-ray Scattering from Oriented Durham Polyacetylene: Structural Changes after Electrochemical Doping

Y. B. Moon, M. Winokur, and A. J. Heeger*

Department of Physics and Institute for Polymers and Organic Solids, University of California, Santa Barbara, California 93106

J. Barker and D. C. Bott

British Petroleum Research Centre, Sunbury-on-Thames, England.
Received December 3, 1986

ABSTRACT: We report on X-ray diffraction studies, carried out before and after electrochemical n-type doping and undoping cycles, of stretch-oriented polyacetylene prepared via the Durham method. After a cycle up to 6 mol % doping with Na^+, the structure returns to that of *trans*-$(CH)_x$ with no loss in crystallinity and with only a minimal decrease in coherence length. Cycling to 12 mol % Na^+ or up to 6 mol % K^+ causes a significant reduction in the crystallinity of the sample. The X-ray data from stretch-oriented *trans*-polyacetylene prepared by the Durham and Shirakawa methods show slight differences; although the basic structure is the same, the Durham material is on the average expanded by about 1% transverse to the chain axis. The Durham material has a slightly shorter transverse coherence length (110 Å vs. 125 Å) but has significantly better orientational order. The X-ray data rule out the in-phase arrangement of the bond alteration on the two polyacetylene chains within the unit cell and indicate that the anti-phase configuration is preferred.

I. Introduction

There are a number of methods available for both the synthesis of polyacetylene[1,2] and the subsequent orientation of the resulting material.[3] Of these, the synthesis developed by Feast et al.[4] at Durham University (so-called Durham polyacetylene) offers particular advantages, as noted in a number of recent publications.[5-8]

Partially aligned samples offer a special opportunity for structural studies, since scans in the (*hk*0) plane provide information on the interchain (transverse) packing and order, whereas scans along the (00*l*) direction probe the atomic structure along the polymer chain. Previous X-ray scattering studies of partially oriented polyacetylene synthesized by the Shirakawa method demonstrated high crystallinity and provided detailed information on the crystal structure, including the first determination of the bond-alternation symmetry-breaking parameter[9] (subsequently verified by an elegant NMR experiment[10]). X-ray diffraction measurements demonstrated that the polymer chains are aligned parallel to the fibrils which characterize the morphology of Shirakawa polyacetylene. These results were confirmed by electron diffraction measurements.[11] While the most recent structural data continues to support a monoclinic unit cell with $P2_1/c$ symmetry, the precise relationship between the two polyacetylene chains within the unit cell of the crystal structure is still somewhat controversial with two possible configurations having been proposed, either an in-phase[12] ($P2_1/a$) or an anti-phase[9] ($P2_1/n$) arrangement of the dimerized backbone. Of the two configurations, the anti-phase configuration is thought to be somewhat lower in energy.[13]

The process of doping is structurally demanding, since it involves injection of the dopant species into the polyacetylene structure with associated major rearrangements of the polymer chains.[14-16] There is, however, no information currently available on the effect of doping and undoping on the structure of the neutral polymer. Knowledge of the structural stability of conducting polymers on electrochemical cycling is pertinent to a variety of possible applications (e.g., rechargeable batteries,[17] electrochemical displays,[18] etc.) in which such polymers will be used as reversible electrode materials.

In this paper, we report on the structural changes which arise from electrochemical cycling (doping and subsequent undoping) of oriented Durham polyacetylene. We compare the results before and after electrochemical cycling for a sample which was initially 90% trans with a sample which was initially isomerized to all-trans through heat treatment. We find that although the material is not structurally damaged by Na^+ up to 6 mol % a single cycle up to 12 mol % causes a considerable reduction in the crystallinity of the polymer. In the case of K^+ doping, even a single cycle up to 6 mol % reduces the crystallinity. We also find that there are subtle, but observable, differences between the structure of the Durham material and that of the Shirakawa material. In addition, our results rule out the in-phase arrangement of the bond alternation on the two chains within the unit cell. Detailed analysis of scans along (00*l*) with fully isomerized samples indicates that the anti-phase configuration is preferred.

II. Experimental Technique

The X-ray scattering data described in this paper utilized primarily samples of Durham polyacetylene synthesized and oriented in the British Petroleum Research Centre at Sunbury-on-Thames.[6,19] Both 90% trans and fully isomerized *trans*-polyacetylene samples were prepared by using different conditions of heat treatment: 22 h at 90 °C for the 90% trans sample and 64 h at 100 °C for complete isomerization. Representative scans were also carried out by using stretch-oriented Shirakawa *trans*-$(CH)_x$ so that direct comparisons (using the same instrumentation) could be made.

Initially, structural characterization of the undoped samples was completed. The pristine Durham polyacetylene samples (either 90% trans or fully isomerized) were in the form of long strips, 3 × 50 × 0.01 mm with *c* axis along the long direction. For an X-ray experiment, the sample was folded, while carefully maintaining the orientation, to an ultimate thickness of ~0.2 mm and then mounted into a sealed cell with beryllium windows. All sample handling was carried out in a controlled atmosphere drybox; the $(CH)_x$ samples were never exposed to air. After the cell was mounted and aligned on the goniometer, a series of X-ray diffractometer scans were executed (using Cu Kα radiation from a 1.2-kW X-ray generator fitted with a flat graphite monochromator and analyzer) including equatorial scans (*hk*0), longitudinal scans (00*l*) and rocking curves. Similar scans were carried out by using the thicker (3 × 30 × 0.1 mm) Shirakawa sample which was cut and clamped rather than folded.

A separate piece of the 90% trans pristine Durham polyacetylene sample was transferred into a Teflon electrochemical cell constructed with stainless-steel electrodes. The cell contained electrolyte, sodium metal (as counter electrode), and a separator; the Durham polyacetylene sample was placed in contact with one electrode and the sodium metal with the other. The electrolyte consisted of high purity (99.9+%) $NaBPh_4$ in a 0.2 M solution in THF (tetrahydrofuran) which had been previously purified by

0024-9297/87/2220-2457$01.50/0

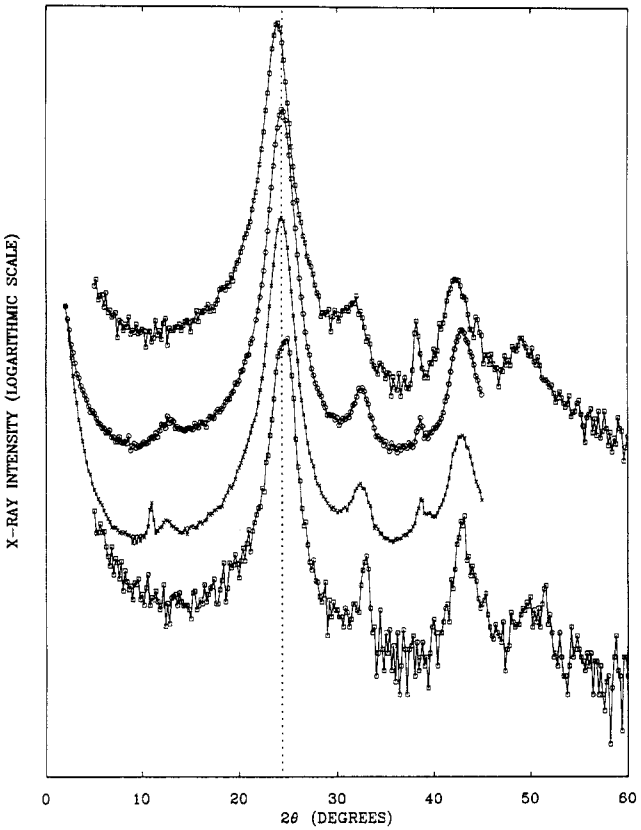

Figure 1. Equatorial (*hk*0) scans (displayed from top to bottom): (1) Durham polyacetylene (90% trans); (2) fully isomerized Durham *trans*-polyacetylene; (3) electrochemically cycled (up to 6 mol % Na^+) Durham polyacetylene; (4) oriented Shirakawa trans-$(CH)_x$. The dotted vertical line at $2\theta = 24.5°$ indicates the position of the main peak of the fully isomerized Durham polyacetylene.

distillation over sodium benzophenone ketyl. Electrolyte volume was kept to a minimum to prevent impurity-induced side reactions. The electrochemical cell was previously calibrated by using electrochemical voltage spectroscopy;[20] well-defined inflections were observed consistent with the results for Shirakawa polyacetylene reported by Shacklette et al.[21] For the neutral sample (prior to doping), the measured open-circuit voltage was 2.3 V; doping to ~5 mol % sodium was accomplished by connecting the cell to a direct current power supply set at 0.85 V and allowing the cell to come to equilibrium over a period of about 48 h. The criteria for equilibrium were final cell current of less than 0.1 μA (compared to an initial short-circuit current of about 1 mA) and a cell voltage drift of only 0.05 V upon disconnection of the external power supply. After equilibrium was reached, the cell voltage was reset at 2.3 V to undope the sample and complete the cycle. Again, equilibrium was established over a 48-h period as verified by using the criteria given above. We note that diffusional modeling of these conditions indicates that doping is not completely homogeneous, but these conditions give acceptable results in a reasonable time scale. After cycling, the Durham polyacetylene sample was transferred into the X-ray cell, and the cell was remounted on the X-ray diffractometer.

A separate set of experiments were carried out in situ during electrochemical doping using thin-wall glass cells. These data provide supplementary information on the effects of electrochemical cycling on the structure. Details of the experimental technique will be reported in a separate paper[22] which focuses on the structural changes which occur as a function of the doping level.

III. Experimental Results

A. Comparison of Results Obtained before and after Electrochemical Cycling. The results from equatorial (*hk*0) scans are presented in Figure 1. The data include the following (displayed from top to bottom): (1) Durham polyacetylene (90% trans), (2) fully isomerized *trans*-DPA, (3) electrochemically cycled (up to 6 mol %) Durham polyacetylene, and (4) oriented Shirakawa *trans*-$(CH)_x$. The Durham polyacetylene scans contain, in addition to the relatively broad peaks from the polymer sample, two weak sharp peaks at $2\theta = 38.6°$ and 44.5°; the latter are unidentified artifacts which have nothing to do with pure polyacetylene. In the cycled Durham polyacetylene scan, one also observes a single sharp Bragg peak at low angle from the electrolyte residue, recrystallized $NaBPh_4$. The complete isomerization of the initially 90% Durham *trans*-polyacetylene by electrochemical cycling (up to 6 mol % Na^+) is evident; the peak positions shift to higher wave vectors that correspond to the positions of the fully isomerized Durham polyacetylene. Although one observes a slight broadening of the peaks and a significant increase in the small angle scattering in the process of cycling (compare the data from the cycled sample, curve 3, with either the pristine 90% trans sample, curve 1, or the pristine thermally isomerized sample, curve 2), the intensities of the peaks are not reduced by cycling up to 6% doping with Na^+. In a separate experiment, a fully (thermally) isomerized Durham polyacetylene sample was cycled. The results were indistinguishable from the data from the initially 90% trans sample (i.e., curve 3). The cycled samples return to the Durham *trans*-polyacetylene structure with only a slight decrease in the transverse coherence length but without significant loss in crystallinity.

Comparing the data from fully isomerized sample (curve 2) and the 90% isomerized sample (curve 1) confirms the expected improvement in structural order. For example, the single peak at $2\theta = 32.5°$ from the (120) reflection is narrower in curve 2, but the splitting of the superposed (110) and (020) at $2\theta = 24.5°$ leads to a broader width.

On comparing the data from the fully isomerized oriented Durham *trans*-polyacetylene sample and the oriented trans Shirakawa sample, one finds significant differences in the peak positions, in the transverse coherence lengths and in the (110)/(020) peak profile. Although the peaks can be indexed identically and have approximately the same intensity ratios, the oriented Durham polyacetylene peaks are all shifted approximately 1% to lower wavevector. For example, the (120) peak from Durham polyacetylene reaches its maximum at $2\theta = 32.5°$, while the corresponding peak position from the Shirakawa sample is at $2\theta = 32.9°$. This direct comparison is somewhat deceptive. Actual determination of the lattice constants, shown in Table I, find that the *a*-axis lattice constant of the Durham samples is approximately 5% larger than that of Shirakawa polyacetylene while the *b*-axis lattice constant is contracted by approximately 1%. The (120) peak and the other higher wavevector peaks are broader in the Durham polyacetylene sample, implying that the transverse coherence length is smaller and that there is greater disorder in the Durham polyacetylene. In addition, the splitting between the overlapping (110) and (020) peaks

Table I
Experimentally Determined Lattice Parameters for Three Types of Durham Polyacetylene (90% Trans, All-Trans, Electrochemically Cycled 90% Trans) and Shirakawa Polyacetylene[a]

	a, Å	*b*, Å	c, Å
Durham polyacetylene (90% trans)	4.24	7.35	2.454 (5)
heat-treated DPA (all-trans)	4.20	7.28	2.456 (5)
electrochemically cycled DPA (90% trans)	4.22	7.30	2.453 (5)
Shirakawa PA	4.05	7.39	2.458 (5)

[a] β is fixed at 91.5°.

is clearer in the scan from the Shirakawa sample, consistent with the better transverse order and the slight difference in lattice parameters. Finally, all-trans Durham samples exhibit weak but measurable scattering near the (010) wavevector, whereas in Shirakawa and Durham polyacetylene (90% trans), this scattering is either absent or undetectable. Given the polymeric nature of polyacetylene, this may indicate the existence of a second phase[23] or greater structural subtlety within the monoclinic phase.

It is not surprising that the oriented Durham polyacetylene product contains structural irregularities. Indeed, it has been shown[24] that these oriented films have conformational defects which derive from the tangled mat of high molecular weight polymer chains in the precursor. By analogy with the orientation of other polymers, it is possible to suggest that the precursor initially gains a pseudonematic order which evolves into a nearly crystalline material at high draw ratios. As evidenced by the observed residual transverse disorder, pristine oriented Durham *trans*-polyacetylene possesses a structure intermediate between nematic and crystalline.

The longitudinal scans through the (002) reflection of the various polyacetylene samples are shown in Figure 2 (using the same top to bottom order as in Figure 1). In contrast to the low wavevector shift of the equatorial reflection positions, the (002) peak of the fully isomerized Durham polyacetylene tends to be at a slightly higher wavevector than that of Shirakawa polyacetylene. Any shift in peak position due to thermal or electrochemical isomerization (from 90% to all trans) of Durham polyacetylene is within the instrumental resolution of ~0.1°. Gaussian fits to the leading edge of the (002) peaks result in estimated longitudinal coherence lengths (using the Sherrer equation convoluted with the instrumental resolution) of 95 Å (Durham polyacetylene, 90% trans), 110 Å (thermally isomerized Durham *all-trans*-polyacetylene), 95 Å (Durham polyacetylene electrochemically cycled to 6 mol % Na^+), and 125 Å (oriented Shirakawa polyacetylene). The Durham polyacetylene sample is slightly less well-ordered along the chain axis, consistent with the results from the transverse scans.

Rocking curves yield a mosaic spread (fwhm) of approximately 10° for the oriented Durham polyacetylene and approximately 35° for the oriented Shirakawa material; the orientation of the Durham polyacetylene is significantly better. As a result, although the longitudinal coherence length is greater in the Shirakawa material, the scans in Figure 2 exhibit "leakage" contributions on the high wavevector side of the (002) which are absent from the Durham polyacetylene scans. These arise from the broadened off-axis scattering; i.e., from (022) and (112) Bragg scattering.

B. In Situ Measurements Carried Out during Electrochemical Doping. Parallel experiments carried out on oriented Durham polyacetylene during in situ with the sample inside a thin-wall glass electrochemical cell provide supplementary information on the effect of electrochemical cycling on the Durham polyacetylene. As a result of the in situ configuration, the diffraction scans (see Figure 3) contain broad scattering peaks from the glass and the solvent inside the cell in addition to the rather sharp peaks diffracted from the polyacetylene sample.

Figure 3a displays a set of equatorial (*hk*0) scans from an oriented pristine Durham polyacetylene sample, the same sample after a cycle up to 6 mol % Na^+ doping and the same sample after subsequent cycle up to 12 mol % Na^+, arranged from top to bottom, respectively. The data before and after doping to 6 mol % Na^+ are the same,

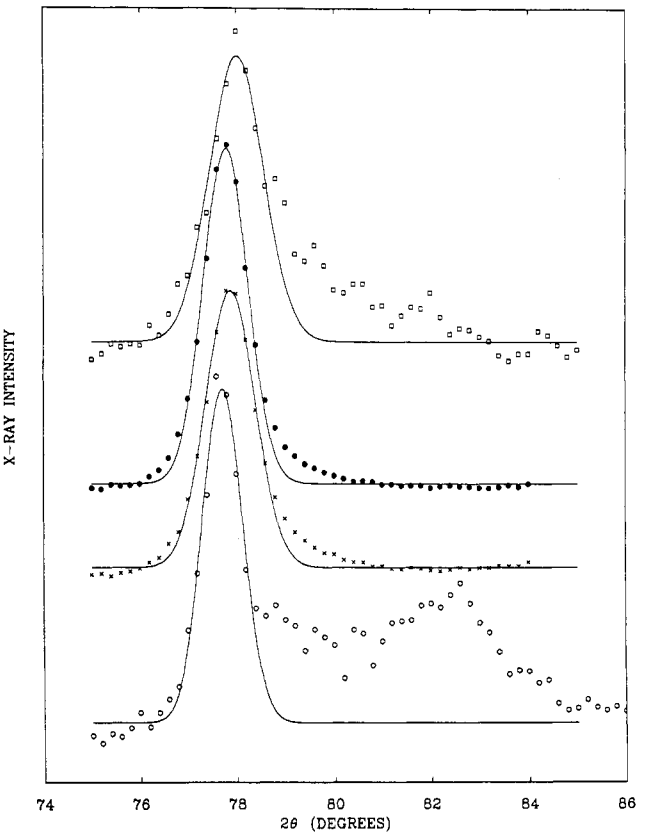

Figure 2. Longitudinal (00*l*) scans around (002) displayed in the same order as Figure 1.

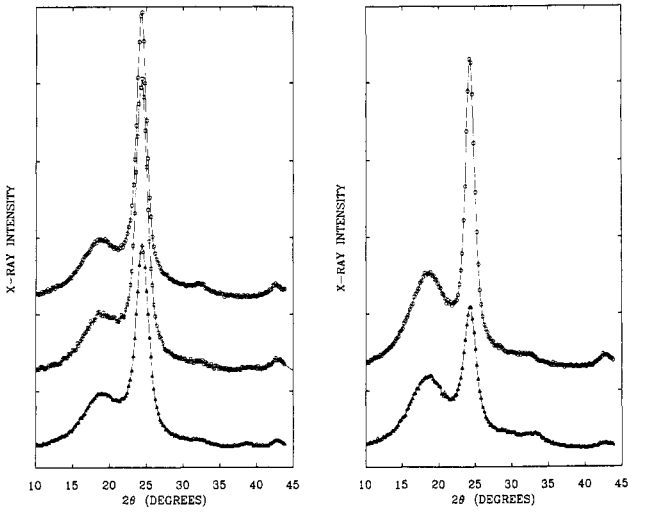

Figure 3. Equatorial (*hk*0) scans from in-situ experiment. (a) From top to bottom: (1) pristine Durham polyacetylene; (2) the same sample after cycling up to 6 mol % Na^+; (3) the same sample after cycling up to 12 mol % Na^+. (b) From top to bottom: (1) pristine Durham polyacetylene; (2) the same sample after cycling to 6 mol % K^+.

consistent with the results described in section IIIA. However, after a cycle to 12 mol % Na^+, there is a significant reduction in the Bragg peak intensities, indicative of a partial loss of crystallinity. It is interesting to compare these results with data from K^+ which has a larger ionic radius. Equatorial scans from a K^+ doping cycle are shown in Figure 3b; in the case of the larger ion, even doping to 6 mol % leads to a significant decrease in crystallinity and obvious changes in the relative peak heights and positions. In this case, it is probable that polyacetylene does not revert to its initial structure after electrochemical cycling. This result is not completely unexpected in view of the fact

that potassium causes more extreme deformations of the polymer chains.

C. Anti-Phase Configuration of the Bond Alternation on Polyacetylene Chains. As a result of the Peierls' distortion, there exists a bond-alternation distortion with magnitude $\pm u_0 = 0.035$ Å projected along the chain direction) in the C–C bond lengths of polyacetylene with respect to the uniform bond length polyene chain. This dimerization would be expected to cause measurable X-ray scattering intensity at the (001) peak position proportional to $(u_0/c)^2$, where c is the c axis lattice constant along the chain direction. However, this reflection is forbidden if the bond alternation patterns on the two $(CH)_x$ chains in the unit cell are out-of-phase. Earlier X-ray studies of Shirakawa polyacetylene by Fincher et al.[9] (although at extremely low count rates) found no measurable intensity at the (001) position, suggesting an anti-phase arrangement. This conclusion has been called into question as a result of an electron diffraction results from Shirakawa material.[11b] However, the possibility of multiple scattering complicates the analysis of low-intensity electron diffraction data. More recently, Leising et al.[12a] reported X-ray results from Durham polyacetylene with observable intensity at (001).

A quantitative demonstration that rules out in-phase ordering requires a direct comparison of the predicted intensity ratio of the (001) peak relative to the (002) peak, $I(001)/I(002)$, with the experimental ratio. Assuming 100% in-phase bond alternation of the two chains in the unit cell and $u_0/c \ll 1$

$$I(001)/I(002) = (\pi u_0/c)^2 F^2 L R$$

where F is the ratio of atomic form factors ($F^2 \approx 3.2$) and L is the ratio of Loretz–polarization factors ($L \approx 4.5$). The effect of sample geometry on the scattering volume at different angles (a factor of 1.1), the effect of the change in instrumental as a function of scattering angle (a factor of 1.2), and the effect of the relatively large mosaic spread of the partially oriented sample (a factor of 4) are all included in the R factor. Since thermal and static Debye–Waller factors and X-ray absorption effects have been ignored in the calculation (both would increase the ratio), the calculated ratio should be considered a lower limit.

The results are summarized in Figure 4; the solid and dashed curves are the calculated (002) and (001) intensities, respectively. The (002) intensity has been fit to the experimental profile (open circles); the calculated (002) and (001) were assumed to have the same width along the (00l) direction. We have also observed weak scattering at the (001) position for oriented Durham polyacetylene, as shown in the inset of Figure 4 (squares). The data from this (001) scan for a fully isomerized Durham polyacetylene sample are also shown in comparison with the experimental (002) and the calculated (001) of Figure 4. Three different Durham polyacetylene samples were carefully scanned near the (001) position to confirm this result. The measured intensity ratio, $I(001)/I(002)$, is significantly less than the value ($\sim 1/9$) reported by Kahlert et al.[12b] The weak (001) scattering inevitably *decreases* either after complete isomerization of 90% *trans*-polyacetylene samples or after electrochemical cycling of all-trans material. These experimental results imply that as the Durham polyacetylene approaches the all-trans isomer, the exent of in-phase coherence decreases. The residual (001) in the Durham polyacetylene results either from strains within anti-phase regions or from traces of domains with in-phase bond alternation.

Since the assumption of in-phase ordering is not consistent with the experimental data, we see only two possibilities: (i) the bond alternation on the two chains within the unit cell are ordered in the anti-phase configuration; (ii) the bond alternation patterns on the $(CH)_x$ chains are essentially random. In this case, there is no net projected c-axis density modulation with period c and thus the (001) scattering intensity would be zero. Although the (002) intensity corresponding to the zigzag polyacetylene chains is found experimentally to be a peak (implying three-dimensional order with a moderate mosaic spread due to incomplete alignment), the bond alternation pattern could in principle be random. However, Fincher et al.[9] were able to correctly obtain the bond alternation distortion parameter (u_0) from analysis of the allowed (hkl) reflections with $l = 1$. The agreement between the experimental and calculated line shapes and intensities demonstrates the existence of coherent interchain order for the bond alternation pattern and thereby rules out the second of the two alternatives listed above.

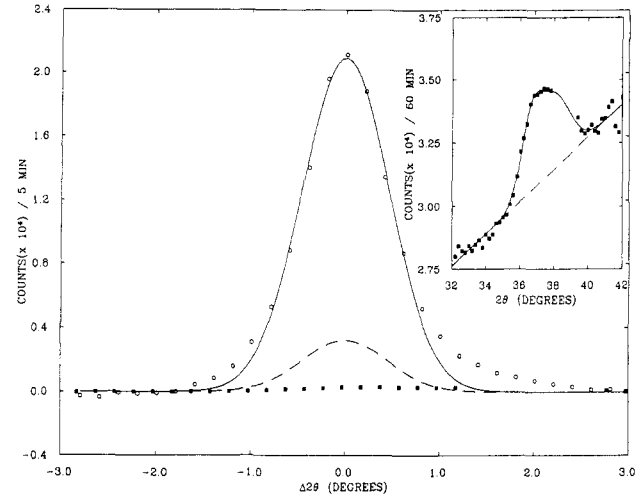

Figure 4. Intensity comparison between (002) and (001) peaks of fully isomerized Durham polyacetylene: open circles, (002) peak with Gaussian fit (solid curve); solid squares, scan through vicinity of (001); dashed line, calculated (001) peak assuming in-phase configuration (see text). The (001) data were checked for three independent samples; typical results are shown on an expanded scale in the inset with the background (dashed curve) indicated.

IV. Conclusions

We have carried out a structural study of polyacetylene, synthesized and oriented by using the Durham route, using X-ray diffraction techniques. The focus of this study was to clarify structural changes arising from electrochemical cycling (doping and undoping) of oriented Durham polyacetylene. We find that after cycling up to 6 mol % with Na^+ the structure returns to that of the pristine sample without loss of crystallinity. After cycling to sufficiently high doping levels (12 mol % for Na^+ ions or 6 mol % for the larger K^+ ions), a decrease in the Bragg peak intensities is observed (indicative of a decrease in crystallinity). We conclude that both the doping level and the dopant size play important roles in the structure after electrochemical cycling. Although some loss of crystallinity is observed, the polymer is remarkably robust and, in the case of Na doping, it returns to the original *trans*-$(CH)_x$ structure even after doping to relatively high levels. Finally, our X-ray results rule out the in-phase arrangement of the bond alternation on the two polyacetylene chains within the unit cell. The X-ray scattering data indicate that the anti-phase configuration is preferred.

Acknowledgment. The X-ray scattering studies were carried out at UCSB and were supported by the Office of

Naval Research. J.B. and D.C.B. thank BP for permission to publish this paper.

Registry No. Na, 7440-23-5; K, 7440-09-7; poly(1,2-ethenediyl), 26571-64-2.

References and Notes

(1) (a) Shirakawa, H.; Ikeda, S. *Polym. J.* **1971**, *2*, 3. (b) Ito, T.; Shirakawa, H.; Ikeda, S. *J. Polym. Sci.* **1974**, *12*, 11.
(2) Luttinger, L. B. *J. Org. Chem.* **1962**, *27*, 1591.
(3) Leising, G. *Polym. Bull.* **1984**, *11*, 401.
(4) (a) Edwards, J. H.; Feast, W. J. *Polym. Commun.* **1980**, *21*, 595. (b) Edwards, J. H.; Feast, W. J.; Bott, D. C. *Polymer* **1984**, *25*, 395.
(5) Bott, D. C.; Chai, C. K.; Edwards, J. H.; Feast, W. J.; Friend, R. H.; Horton, M. E. *J. Phys. (Les Ulis, Fr.)* **1983**, *44*(C3), 143.
(6) White, D.; Bott, D. C. *Polym. Commun.* **1984**, *25*, 98.
(7) Bott, D. C. *Polym. Prepr. (Am. Chem. Soc., Div. Polym. Chem.)* **1984**, *25*, 219.
(8) (a) Horton, M. E.; Bradley, D. D. C.; Friend, R. H.; Chai, C. K.; Bott, D. C. *Mol. Cryst. Liq. Cryst.* **1985**, *117*, 51. (b) Bott, D. C.; Brown, C. S.; Winter, J. N.; and Barker J. *Polymer* **1987**, *28*, 601.
(9) Fincher, C. R.; Chen, C. E.; Heeger, A. J.; MacDiarmid, A. G.; Hastings, J. B. *Phys. Rev. Lett.* **1982**, *48*, 100.
(10) Yannoni, C. S.; Clarke, T. C. *Phys. Rev. Lett.* **1983**, *51*, 1191.
(11) (a) White, D.; Bott, D. C.; Weatherhead, R. H. *Polym. Commun.* **1983**, *24*, 805. (b) Chien, J. C. W.; Karasz, F. E.; Shimamura, K. *Makromol. Chem., Rapid Commun.* **1982**, *3*, 655.
(12) (a) Leising, G.; Kahlert, H.; Leiter, O. *Springer Ser. Solid-State Sci.* **1985**, *63*, 56. (b) Kahlert, H.; Leitner, O.; Leising, G. Proc. ICSM 1986, Kyoto, June, 1986; *Synth. Met.* in press.
(13) Baeryswyl, D.; Maki, K. *Phys. Rev. B: Condens. Matter* **1983**, *28*, 2068.
(14) (a) Baughman, R. H.; Murthy, N. S.; Miller, G. G. *J. Chem. Phys.* **1983**, *79*, 515. (b) Baughman, R. H.; Shacklette, L. W.; Murthy, N. S.; Miller, G. G.; Elsenbaumer, R. B. *Mol. Cryst. Liq. Cryst.* **1985**, *118*, 253.
(15) Shacklette, L. W.; Murthy, N. S.; Baughman, R. H. *Mol. Cryst. Liq. Cryst.* **1985**, *121*, 201.
(16) Wieners, G.; Weisenhofer, R.; Monkenbusch, M.; Stamm, M.; Leiser, G.; Enklemann, V.; Wegner, G. *Makromol. Chem., Rapid Commun.* **1985**, *6*, 425.
(17) MacInnes, D., Jr.; Druy, M. A.; Nigrey, P. A.; Nairns, D. P.; MacDiarmid, A. G.; Heeger, A. J. *J. Chem. Soc., Chem. Commun.* **1981**, 317.
(18) (a) Druy, M. A.; Seymour, R. J. *J. Phys. (Les Ulis, Fr.)* **1983**, *44*(C3), 595. (b) Kobayashi, M.; Colarneri, N.; Boysel, M.; Wudl, F.; Heeger, A. J. *J. Chem. Phys.* **1985**, *82*, 5717.
(19) Bott, D. C.; Walker, N. S.; White, D.; Friend, R. H.; Townsend, P. D. *Mol. Cryst. Liq. Cryst.* **1985**, *117*, 95.
(20) (a) Thompson, A. H. *Physica B+C (Amsterdam)* **1980**, *99B+C*, 100; *Phys. Rev. Lett.* **1978**, *40*, 1517. (b) Kaufman, J. H.; Chung, T.-C.; Heeger, A. J. *Electrochem. Soc.* **1984**, *131*, 2847. (c) Barker, J.; Walker, N. S.; Baldwin, D. I.; Bott, D. C., to be submitted for publication.
(21) (a) Shacklette, L. W.; Toth, J. E.; Murthy, N. S.; Baughman, J. *Electrochem. Soc.* **1985**, *132*, 1529. (b) Shacklette, L. W.; Toth, J. E. *Phys. Rev. B: Condens. Matter* **1985**, *32*, 5892.
(22) Winokur, M.; Moon, Y. B.; Heeger, A. J.; Barker, J.; Bott, D. C.; Shirakawa, N. *Phys. Rev. Lett.* **1987**, *58*, 2329.
(23) Dickinson, L. C.; Hirsch, J. A.; Karasz, F. E.; Chien, J. C. W. *Macromolecules* **1985**, *18*, 2374.
(24) Friend, R. H.; Bradley, D. D. C.; Pereira, C. M.; Townsend, P. D.; Bott, D. C.; Williams, K. P. J. *Synth. Met.* **1985**, *13*, 101.

The Role of Oxygen in the Photoaging of Bisphenol A Polycarbonate. 2.† GC/GC/High-Resolution MS Analysis of Florida-Weathered Polycarbonate

A. Factor,* W. V. Ligon, and R. J. May

General Electric Company, Corporate Research & Development Center, Schenectady, New York 12301. *Received March 19, 1987*

ABSTRACT: Use of GC/GC/high-resolution mass spectrometry to analyze the $LiAlH_4$ and $LiAlD_4$ reductive cleavage products from a 4-year Florida-aged sample of non-UV-stabilized bisphenol A polycarbonate has confirmed the presence of small amounts of photo-Fries and ring oxidation products along with large amounts of side-chain oxidation products. These results are consistent with a photoaging mechanism in which side-chain and ring photooxidation are initiated by a photo-Fries process and colored photoproducts are derived primarily from ring oxidation.

Introduction

When non-UV-stabilized bisphenol A polycarbonate is exposed outdoors for several years, its surface is observed to become yellow and show evidence of cross-linking, pitting, and cracking. Most early investigations[1-8] on the photoaging of bisphenol A polycarbonate suggested that the key mechanism in this phenomenon is the photo-Fries reaction (Scheme I). More recent work,[9-16] however, indicates that under the influence of longer wavelengths of light—such as experienced during outdoor exposure—photooxidation (Scheme II) is the predominant reaction pathway. In addition, work by Lemaire[13,14] demonstrated that photo-Fries products are themselves easily photooxidized, making it difficult to find evidence of the photo-Fries pathway.

Although the evidence has been less rigorous, ring oxidation has been shown to play a role in the photoaging of bisphenol A polycarbonate. For example, ESCA studies of resin photooxidized under both sunlight ($\lambda > 300$ nm)[11] and Hg arc light ($\lambda > 280$ nm)[10,12] show a decrease of the $\pi \rightarrow \pi$ shake-up ESCA satellite, indicating the loss of aromatic groups. Quantitative FTIR analyses of laser-induced polycarbonate photodegradation[16] indicate a depletion of main-chain aromatic groups and suggest an increase in ring substitution. Oxygen uptake experiments[9] indicate the absorption of up to 12 mol of O_2 per monomer unit and the evolution of 4.6–7.7 mol of $CO + CO_2$ per monomer unit during the photooxidation of thin polymer films using different light sources. These high values cannot be explained by side-chain oxidation and carbonate group hydrolysis alone and indicate that ring oxidation is also occurring. Finally, both outdoor and artificial weathering experiments of the side-chain-free poly-

† The paper cited in ref 9 is considered to be part 1 of this series.

0024-9297/87/2220-2461$01.50/0